Title: Chemically Functionalized Conical PET Nanopore for Protein Detection at the Single-molecule Level

Author: Youwen Zhang[a], Xiaohan Chen[a], Ceming Wang[b], Golbarg M Roozbahani[a], Hsueh-Chia Chang[b], and Xiyun Guan[a,*]

Author affiliation:

[a] Department of Chemistry, Illinois Institute of Technology, 3101 S Dearborn St, Chicago, IL 60616, USA

[b] Department of Chemical and Biomolecular Engineering, University of Notre Dame, Notre Dame, IN 46556, USA

*Corresponding author:

Xiyun Guan

Department of Chemistry

Illinois Institute of Technology

3101 S Dearborn St, Chicago, IL 60616, USA

Tel: 312-567-8922; Fax: 312-567-3494

E-mail: xguan5@iit.edu

Chemically Functionalized Conical PET Nanopore for Protein Detection at the Single-molecule Level

ABSTRACT

Proteins are essential for all living organisms, and perform a wide variety of functions in the cell and human body, including structural, mechanical, biochemical, and signaling. Since proteins can serve as valuable biomarkers for health status and diseases states, and enable personalized medicine, sensitive and rapid detection of proteins is of paramount importance. Herein, we report a chemically functionalized conical shaped poly-(ethylene terephthalate) nanopore (PET nanopore) as a stochastic sensing element for detection of proteins at the single-molecule level. We demonstrate that the PET nanopore sensor is not only sensitive and selective, but also can differentiate proteins rapidly, offering the potential for label-free protein detection and characterization. Our developed PET nanopore sensing strategy not only provides a general platform for exploring fundamental protein dynamics and rapid detection of proteins at the single-molecule level, but also opens new avenues toward advanced deeper understanding of enzymes, development of more efficient biosensing technologies, and constructing novel biomimetic nanopore systems.

Keywords: Solid-state nanopore, PET film, HIV-1 Protease, Trypsin, Proteins.

INTRODUCTION

Proteins are important macromolecules, which are made up of long chains of amino acids. These large biomolecules are essential for all living organisms, and perform a wide variety of functions in the cell, including providing structural support, catalyzing chemical reactions, storing nutrients and providing energy, responding to stimuli, transporting molecules throughout human body, and acting as messengers to control or regulate specific physiological processes (Keskin et al. 2016). Accordingly, a change in protein structure and/or concentration underlies a wide variety of physiological and pathological processes. Since proteins can serve as valuable biomarkers for health status and diseases states, and

enable personalized medicine, sensitive and rapid detection of proteins is of paramount importance. At present, there are two major protein detection / characterization approaches. The first one is affinity-based assay such as ELISA and various formats of immunoassays including biosensors (García-Chamé et al. 2020; Ilkhani et al. 2015; Zhang et al. 2020), where an antibody is usually employed (Xie et al. 2009) to detect protein abundance. The second one is to directly determine the protein's structure and composition. Several examples of such methods include X-ray crystallography (Smyth and Martin 2000), nuclear magnetic resonance spectroscopy (Bovey 1961), and circular dichroism (Greenfield 2006). In spite of their wide utility in protein quantification and characterization, one major limitation of these methods is that they are not suitable for use to obtain dynamic structural information (e.g., conformational change) of a single protein in real time. Note that protein dynamics plays a critical role in its function, including ligand binding, enzyme catalysis, protein-protein interaction, and so on.

One emerging technique, which has been utilized to detect protein abundance (Chuah et al. 2019), investigate protein structure (Talaga and Li 2009), and study protein function (Chen et al. 2019), is nanopore stochastic sensing. By taking advantage of the ionic current modulations produced by the passage of target analytes through a single nanoscale-sized channel as a result of diffusion, electrophoretic force, and electroosmotic flow, nanopore sensor can detect analytes at the single-molecule level (Chen et al. 2019). Due to its label-free and amplification-free advantages, nanopore technology has been utilized as a versatile tool to study a variety of topics, including biosensing (Chen et al. 2018; Roozbahani et al. 2019; Wang et al. 2018) and especially DNA sequencing (Bayley 2017; Branton et al. 2008; Deamer et al. 2016; Heerema and Dekker 2016). To date, there are mainly two types of nanopore technology: biological protein nanopore and synthetic solid-state nanopore. While biological nanopores offer better resolution/sensitivity and have been successfully utilized to study a variety of topics as described above, they are limited to very specific operational conditions due to the fragility nature of the supporting lipid bilayer. In contrast, although solid-state nanopores are in principle more stable, and are more appropriate for field-deployable applications, the current synthetic nanopore technique has limited sensor application due to the much larger background noise and

significantly worse sensitivity / resolution of the solid-state nanopores over the protein pores. Therefore, development of sensitive and high-throughput synthetic nanopore sensors have attracted increasing interest in the recent years (Karawdeniya et al. 2018; Shim et al. 2013; Siwy and Davenport 2010; Storm et al. 2005). The poly-(ethylene terephthalate) films (PET) were among the earliest membranes used for constructing synthetic nanopores due to many advantages such as their commercially availability, cost-effectiveness, ease to transport, and high stability. Furthermore, it is does not require complicated procedure to make single track-etched conical shaped nanopore. However, due to the poor resolution and sensitivity (which is in large part attributed to lack of properly designed inner surface functions), they were rarely used as single-molecule stochastic sensing elements for sensor applications. At present, PET nanopores take advantage of changes in the current-voltage curves and use a steady-state approach to detect analytes (Ali et al. 2011a), which involves the response of the nanopore to numerous analyte molecules. Herein, we report a chemically functionalized PET nanopore for stochastic detection and characterization of proteins at the single-molecule level.

Experimental Section

Materials and Reagents.

HIV-1 protease was ordered from BioVendor Lab (Brno, Czech Republic), while enhanced green fluorescent protein (EGFP) was purchased from BioVision, Inc. (Milpitas, CA, USA). All the other chemicals and proteins, including bovine serum albumin (BSA), human serum albumin (HSA), and trypsin (from bovine pancreas) were obtained from Sigma-Aldrich (St Louis, MO). All the proteins and chemicals were dissolved in HPLC-grade water (ChromAR, Mallinckrodt Baker). The stock solutions of proteins were prepared at 200 μg/mL each and kept at −20 °C before and after immediate use, while HIV-1 protease was prepared at a concentration of 200 μg/mL and stored at −80 °C before and after use. MES buffer (containing 100 mM 4-morpholineethanesulfonic acid, pH 6.0) was used in chemical modification of PET nanopore. Electrolyte solutions used in this work contained 1.0 M KCl, 10 mM Trizma base and 1 mM EDTA, with the solution pH adjusted ranging from 3.5 to 7.5.

Fabrication of the conical shaped polymeric nanopore. Details on the fabrication of single asymmetric nanopores in polyethylene terephthalate (PET) membrane have been described previously (Wang et al. 2015). Briefly, the 12 μm thick polyethylene terephthalate (PET) foils were irradiated with single swift heavy ions (Au) with energy of 11.4 MeV per nucleon at the GSI in Darmstadt, Germany. An irradiated foil was subsequently etched at room temperature (295 K) by an asymmetric etching method, where the foil was mounted between two isolated containers that contained an etchant solution of 2.5 M NaOH in 1:1 MeOH/H_2O and a stopping solution of 1 M HCOOH and 1 M KCl aqueous solution, respectively. The etching process started from one side of the PET foil, but was immediately stopped when etched through and as a result, a single conical nanopore was formed on each irradiated PET foil. The addition of methanol in the etching solution could enlarge the cone angle of the conical nanopores. A secondary symmetric etching process (2 M NaOH) was applied to enlarge the tip size. In all cases, the diameter of the base was around 1000 ± 80 nm, as determined by electron microscopy (Scheme 1). The final tip diameter was ~5.6 nm, which was determined by an electrochemical method using the equation (Hou et al. 2009) shown as below:

$$d_{tip} = \frac{4GL}{\pi\kappa D}$$

Where d_{tip} is the tip diameter, D is the base diameter (D = 1 μm), and κ is the special conductivity of the electrolyte. For 1 M KCl solution at 25 °C, κ is 0.11173 $\Omega^{-1}cm^{-1}$. L is the length of the channel, which is approximated to the thickness of the membrane after chemical etching (11.5 μm). G is the conductance in 1 M KCl solution (G = 4.3 $n\Omega^{-1}$) and was calculated from the produced ionic current at an applied voltage bias ranging from -100 mV to +100 mV (Figure S1).

Modification of the PET nanopore. Attachment of ethylenediamine to the carboxyl group on the conical nanopore's surface was achieved by using a 2-step coupling method (Zhang et al. 2019). First, the PET film was immersed in a MES buffer solution (pH 6.0) containing 20 mM 1-ethyl-3-(-3-dimethylaminopropyl) carbodiimide hydrochloride (EDC) and 100 mM *N*-hydroxysulfosuccinimide (Sulfo-NHS) for 60 min under an ice-water bath. Then, 50 mM of ethylenediamine was added to the PET nanopore base side solution (Figure S2)

for 8-h at room temperature for coupling amide group after previous solution was discarded. The functionalized PET film was stored for 24 h in the KCl buffer (pH 7.5, 26 °C) before further experiments.

Electrochemical recording and data analysis. Unless otherwise noted, all the experiments were performed under symmetrical buffer conditions with a 3.0 mL solution comprising 1 M KCl, and 1 mM EDTA (pH 7.5) at 26 ± 1 °C with an applied voltage bias (via a pair of Ag/AgCl electrodes) ranging from -1 V to 1 V. All the proteins were added to the base compartment, while the nanopore tip side was connected to "ground". Currents were recorded with a patch clamp amplifier (Axopatch 200B, Molecular Devices; Sunnyvale, CA, USA), and all the data were analyzed with pClamp 10.7 (Molecular Devices), with the conductance and τ_{off} values obtained according to our previous work (Wang et al. 2013). Each single-channel current trace was recorded for at least 1 minute. Fluorescence spectra were obtained at λex/em = 488/507 nm by using a luminescence spectrophotometer (LS50B, PerkinElmer, Waltham, MA, USA).

Results and Discussion

Chemically functionalized PET nanopore with amine terminates at *base*-side.
According to the literature, three conditions need to be satisfied in order to observe ionic current modulations caused by the translocation of biomolecules in the nanopore. These include : 1) the size of the analyte and the diameter of the nanopore should be comparable with each other (Vlassiouk et al. 2009); 2) the analyte translocation velocity has to be slow enough for the recording instrument to pick up the event signal (Plesa et al. 2013; Roman et al. 2017); and 3) the energetic barrier determined by both electrostatic interactions and geometrical restrictions in a confined volume needs to be overcome (Slonkina and Kolomeisky 2003). Previous studies with PET nanopores showed that, when protein molecules were added to the unmodified PET nanopores, they could not produce frequent current modulations but instead might cause a change in the open channel current. One likely interpretation is that proteins could not pass through the nanopore, which is either attributed to the large entropic barrier due to the size of the nanopore or because of their

adsorption onto the outside surface or within the pore (Ali et al. 2008; Sexton et al. 2007) (note that the unmodified PET membrane has a large negative charge density (Vlassiouk and Siwy 2007)). In order to utilize PET nanopores as single-molecule stochastic sensing elements to detect proteins, we produced an asymmetrically modified single conical PET nanopore by covalently attaching amine groups onto the inner surface (bearing carboxylic groups) of the track-etched PET nanopore at the *base* side (i.e., the larger opening of the fluidic channel). We reduce the entropic barrier by driving the proteins from the base side with a much larger cross-section area and use amine-modification to significantly reduce the negative charge density at the entry end to minimize adsorption (Henrickson et al. 2000) (Scheme 1). The relatively non-uniform (discrete) charge surface of the modified PET nanopore could reduce the intrapore electric field and slow down the biomolecular translocation velocity. The lower electric field would be a result of reducing intrapore ion depletion action due to the conic geometry and the associated conductivity gradient (Yan et al. 2013). Conversely, the amine modification may enhance the intrapore electric field if it creates a bipolar pore that can also induce intrapore ion depletion (Ali et al. 2008; Ali et al. 2010; Vlassiouk et al. 2009). Adsorbed proteins can cause aggregation and clogging (Wang et al. 2015). The higher field introduced by the depletion action can then favor rapid desorption such that adsorption can still be tolerated. We scrutinize these important issues of amine-functionalized conic nanopore with several experiments.

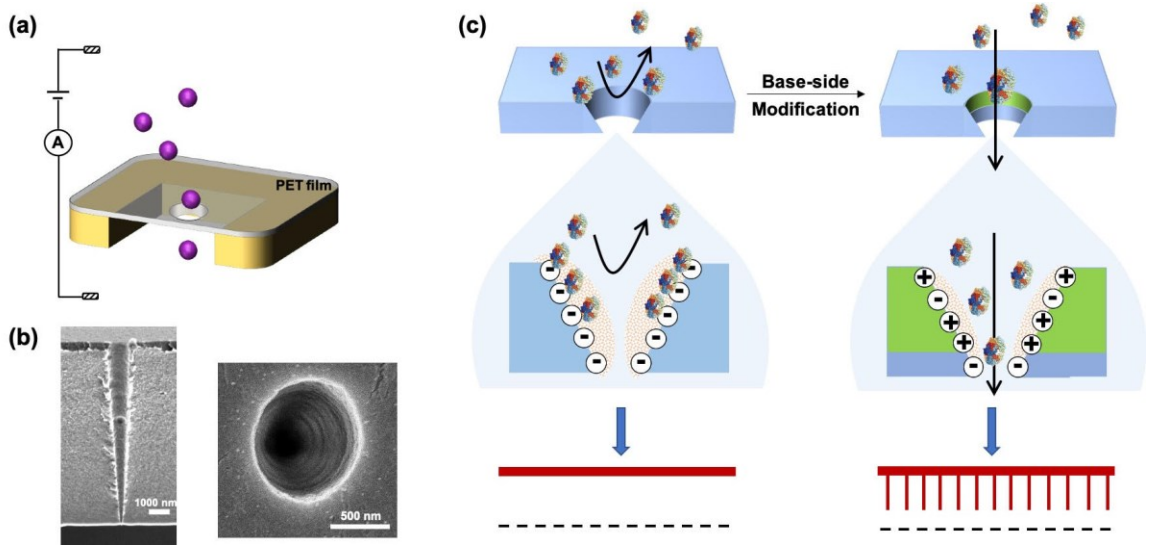

Scheme 1. The principle of a modified single conical PET nanopore for detection of proteins. (a) Schematic representation of the PET nanopore sensing system; (b) Representative cross-sectional SEM image and top view of a conical nanopore; (c) Before modification of the PET nanopore, protein molecules could not pass through the nanopore due to the large energy barrier, and some protein molecules might be absorbed on the interior wall of the nanopore by electrostatic and hydrophobic interactions. In contrast, asymmetric modification of the nanopore *base* produces a new type of surface and property in the interior wall of the nanopore, which reduces the energetic barrier for proteins' entrance into the pore and slows down the velocity of ion flux, resulting in ionic current blockage events.

The current-voltage (I-V) curves of the PET nanopore bathed in a 1 M KCl electrolyte solution of pH 7.5 were displayed in Figure 1. Clearly, compared with the non-modified PET nanopore, the open channel currents of the amine-modified PET nanopore decreased significantly at applied positive potentials, while increased slightly at negatively applied voltage biases. The changes in the I-V characteristics of the PET nanopore before and after ethylenediamine modification confirmed the successful ethylenediamine immobilization to the nanopore inner surface wall. Furthermore, we noticed that chemical modification of the interior surface of the PET nanopore had a significant effect on its ionic transport properties. For example, the asymmetrically modified PET nanopore bipolar diode produced a larger rectification ratio (which is defined as the absolute value of the current obtained at -1 V divided by the current at +1 V) than the unmodified PET unipolar diodes with homogeneous surface charges (1.37 vs. 1.19). Since the conical PET nanopore has deprotonated carboxyl groups and hence was cation selective, it could rectify the ionic current with the preferential flow of cations from the wider base side to the narrower tip (Ali et al. 2011b; Choi et al. 2006). In contrast, after modification with amines, the PET pore was relatively positively charged at the *base* side, and therefore became less cation selective than the unmodified one. The rectification phenomenon of a conic pore can be due to the conic geometry or by the bipolar charge distribution that results from the amine modification (Cervera et al. 2006; White and Bund 2008; Yan et al. 2013).

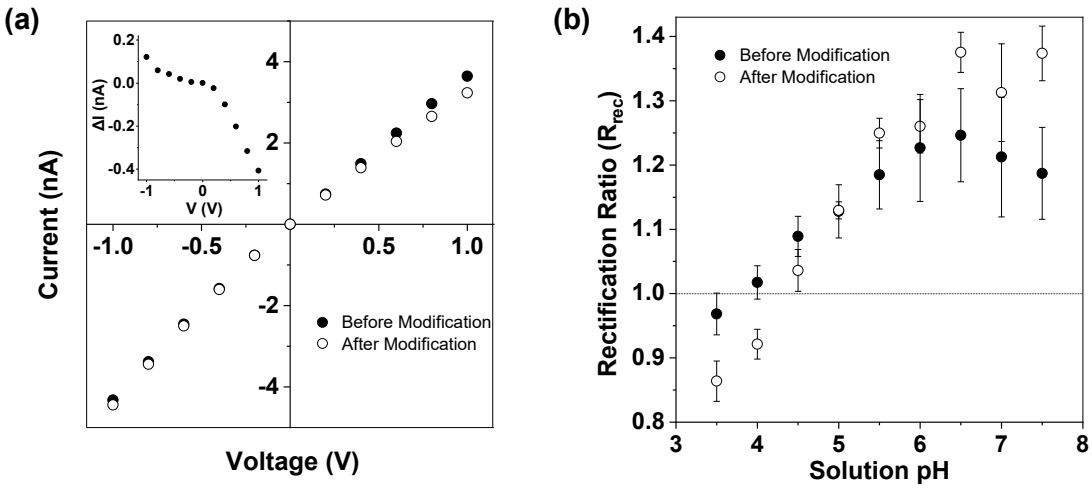

Figure 1. Modification of a single conical PET nanopore. (a) Current-voltage (I-V) curves before and after chemical modification. The inset in Fig. 1a displayed the change in the ionic current before and after nanopore modification. Experiments were performed in a solution containing 1 M KCl and 1 mM EDTA (pH 7.5). The base side of the PET nanopore was modified in 0.1 M MES (pH 6.0), 0.05 M EDC/0.2 M Sulfo-NHS, and 0.05 M ethylenediamine. The diameters of the nanopore tip and base are ~ 5.6 nm and 1000 nm, respectively. (b) Plot of rectification ratio (R_{rec}) as a function of solution pH. The values of R_{rec} were measured at 1 V. The current-voltage curve flipped at the value of pH that corresponds to the film isoelectric point (pI). The value of pI was ~4.3 for the amine-modified PET pore and ~3.8 for the unmodified one, with no rectification at this point.

Since the solution pH affects the net charge of the interior surface (bearing COOH and NH_2 groups) of the PET nanopore, the pH effect on the nanopore ionic transport was further investigated. The current-voltage curves at different electrolyte pH values and the plot of rectification ratio (R_{rec}) of the PET nanopore versus solution pH were depicted in Figure S3 and Figure 1b, respectively. Our experimental results suggested that the isoelectric point of the interior wall of the modified PET pore was ~4.3, while that of the unmodified PET pore was ~3.8, which provided further evidence that ethylenediamine was successfully attached to the surface of the PET film. This conclusion was also supported by the increase in the rectification ratio due to the bipolar charge distribution that results from amine modification of the base.

Detection of HIV-1 Protease

To proof-of-concept demonstrate the utility of the functionalized PET nanopore as a feasible single-molecule stochastic sensing element for detection of proteins, transport of

HIV-1 protease (HIV-1 PR) in the amine-modified PET nanopore was initially investigated at an applied potential bias of 800 mV in an electrolyte buffer solution containing a 1.0 M KCl, 10 mM Trizma base and 1 mM EDTA (pH 7.5). As a control, the interaction between HIV-1 PR and the unmodified PET pore was also studied under the same experimental conditions. Note that HIV-1 PR is essential for the life cycle of the human immunodeficiency virus as it cleaves newly synthesized polyproteins (e.g., Prgag and Prgag-pol) to create the mature protein components of infectious HIV virions (Zhang et al. 2018). Our experiments showed that, HIV-1 PR did not produce any observable current modulation events in the unmodified PET nanopore no matter they were added to either the tip (data not shown) or the base side (Figure 2a). Instead, the open channel current decreased by 62 pA after the protein was added to the electrolyte solution. One likely interpretation is that the unmodified PET nanopore is cation selective so that the cationic HIV-1 PR molecules would be absorbed on the interior wall of the nanopore (Ali et al. 2008) by electrostatic interactions, resulting in the negatively charged surface density diminished locally. In contrast, when HIV-1 PR was added to the base side of the amine-modified nanopore, downward current blockage events appeared in the current trace at a positively applied voltage bias (Figure 2b). Furthermore, with an increase in the concentration of the added protein, more frequent events were observed (Figure 2c), a clear indication that these events were attributed to the interaction between HIV-1 PR and the PET nanopore. Similar to the previous studies on the molecular transport through a nano-channel (Chen et al. 2018), statistical data analysis showed that these downward current modulations could be categorized into two types. One type of events showed a much smaller mean residence time (0.93 ± 0.14 ms vs. 114.2 ± 19.4 ms) and a smaller blockage amplitude than the other type (Figures 2d - 2g). Clearly, the smaller duration events were more likely due to the short residency (e.g., collision) of the HIV-1 PR protein in the PET nanopore, while the longer-lived ones were attributed to the translocation of the protein molecules from the base of the nanopore to the tip side. The Poisson distribution of the residence time (Figs. 2f and 2g), with a residence time minimum much higher than the instrumentation cutoff, suggests that there is reversible adsorption, which would be

supported by further analysis of this Poisson distribution with respect to the applied voltage.

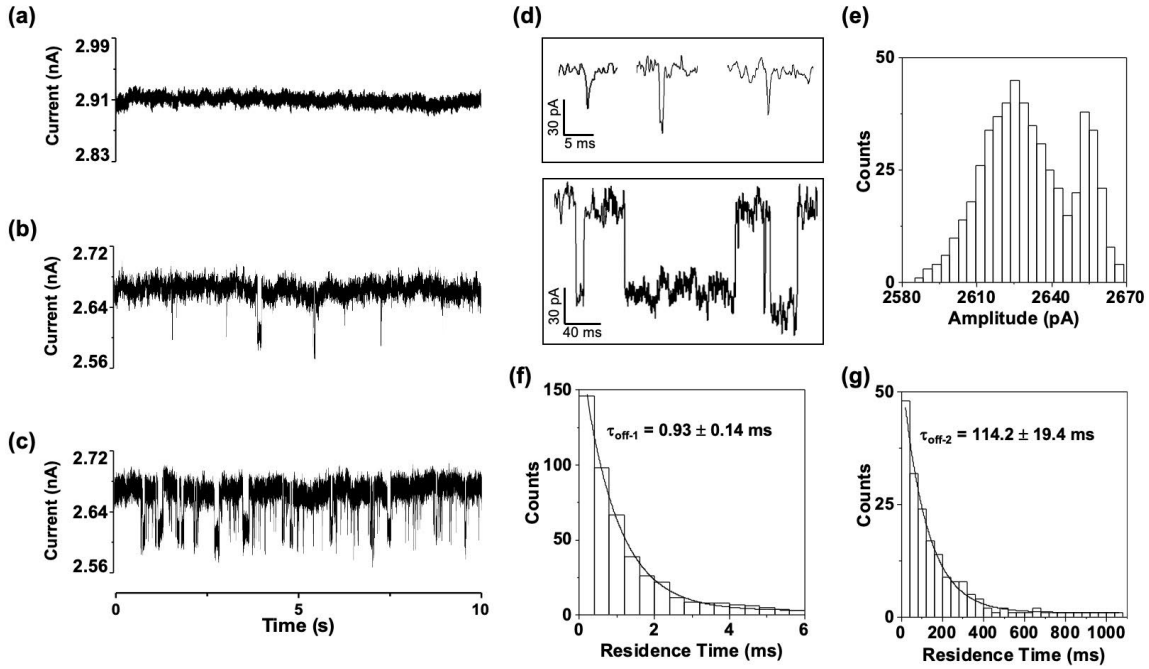

Figure 2. Detection of HIV-1 protease in a PET nanopore. Typical 10-s single channel recording trace segments of a) 100 ng/mL HIV-1 protease in the unmodified PET nanopore, b) 10 ng/mL and c) 100 ng/mL HIV-1 protease in the amine-modified PET nanopore; d) selective individual short-lived and long-lived events; and the corresponding event (e) amplitude histogram and residence time histograms of (f) short-lived and (g) long-lived events of Figure 2c. The experiments were performed at +800 mV in a solution comprising 1 M KCl and 10 mM Tris (pH 7.5). An uninterrupted 2-min single-channel recording trace of 100 ng/mL HIV-1 PR in the modified PET nanopore was displayed in Figure S4.

To support that HIV-1 PR could translocate through the PET nanopore, another experiment was performed, where enhanced Green Fluorescence Protein (eGFP), which has a similar diameter (4.2×2.4×2.4 nm vs. 4.5×2.3×2.5 nm) to that of HIV-1 PR, was added to the PET nanopore. Since eGFP has an isoelectric point (PI) of 5.8, it would be negatively charged at pH 7.5. To make sure that the nanopore experiment with eGFP was carried out under a similar condition to that of HIV-1 PR (positively charged at pH 7.5), the investigation was performed in a buffer solution of pH 5.0 instead of pH 7.5, and with 100 ng/mL of eGFP added to the base of the nanopore at the same applied voltage bias of +800 mV. The solution at the nanopore *tip*-side was collected 3-h later, and its fluorescence intensity was measured with λex/em = 488/507 nm at room temperature. As shown in Figure 3, the fluorescence signal of the tip-side compartment solution increases significantly (from 1.9

to 19.3 a.u.) after 3-h eGFP /PET nanopore interaction, indicating the successful translocation of eGFP through the nanopore.

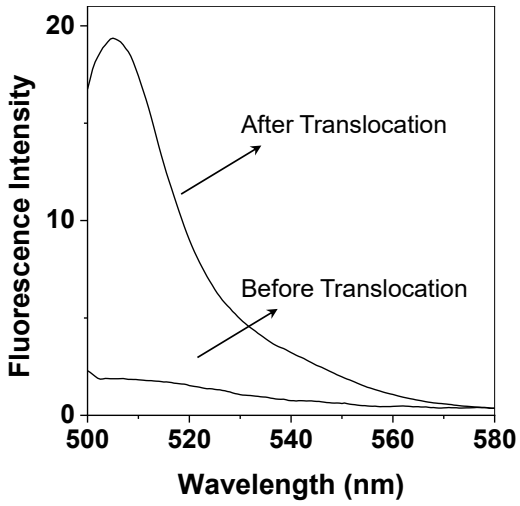

Figure 3. Fluorescence intensity of the nanopore tip-side compartment solution before and after 3-h eGFP translocation in the modified PET nanopore. The experiment was performed at +800 mV with 100 ng/mL of eGFP added to the base side of the modified nanopore bathed in a pH 5.0 electrolyte solution comprising 1 M KCl and 10 mM Tris. The fluorescence spectrum was obtained with $\lambda_{ex/em}$ = 488/507 nm at room temperature.

Voltage effect

Previous studies including ours have shown that the potential applied across the nanopore played an important role in the resolution / performance of the nanopore sensor. In order to find an appropriate voltage bias for sensitive detection of proteins, translocation of HIV-1 PR (100 ng/mL) in the amine-modified PET nanopore was further investigated at a series of potentials ranging from +200 mV to +1000 mV. As shown in Figure 4, at an applied voltage of +200 mV, the ionic current of the PET nanopore was quite stable. In contrast, when the potential increased to +400 mV, current modulation events were clearly observed. After that, with an increase in the applied potential bias, both the amplitude and the frequency of the HIV-1 PR events increased, while the mean residence time decreased. To be more specific, as the voltage increased from +400 mV to +1000 mV, the event mean residual current for HIV-1 PR in the PET pore increased from 16.5 ± 4.3 pA to 125.2 ±

15.2 pA, its residence time decreased from 611.6 ± 142.7 ms to 20.8 ± 7.1 ms, while the event frequency increased from 16.2 ± 2.7 min^{-1} to 80.6 ± 13.8 min^{-1}. Note that the reason why a threshold value of the applied voltage was required for the observation of HIV-1 PR translocation events in the PET nanopore is because the protein molecules needed to overcome an entropic penalty for entering the base side of the PET nanopore from the bulky solution, and this voltage threshold phenomenon has been well documented in the previous experiments with DNA translocation in the biological protein pores (Henrickson et al. 2000). Furthermore, the experimental results regarding the effect of applied voltage bias on the event mean residence time and frequency could be well explained by electrophoretic velocity (V) and electrophoretic flux (J) which are both proportional to the electric field (note that $V=qE/6\pi\eta r$, where E is electric field strength, q and r are the charge and radius of the ion, respectively, and η is the viscosity of the solution; $J=-zFDCE/RT$, where D is the diffusion coefficient and C is the concentration of the ion). Since the electric field strength is directly proportional to the voltage applied, clearly, an increase in the voltage would lead to an increase in the electric field strength and hence an increase in both the electrophoretic velocity and the electrophoretic flux. Accordingly, a decrease in the event residence time and an increase in the event frequency could be expected. Interestingly, we noticed that the lower bound of the Poisson residence time distribution in Fig. 4b seemed to be insensitive to voltage but the upper bound decreased with voltage, as is consistent with the bulk electrophoretic velocity argument for the mean translocation time. This suggests that the slowest and most dominant event involves adsorption, with the rate-controlling adsorption step insensitive to the field. Adsorption still occurs but the adsorbed proteins are quickly removed by the electric field such that aggregation does not occur. We hence achieve both high throughput and long residence time for the PET nanopore sensor. It should be noted that a larger applied voltage bias would lead to more frequent HIV-1 PR events (a ~5 folds increase in the event frequency as the potential increased from +400 mV to +1000 mV), thus offering the PET nanopore a better sensitivity. However, when the applied voltage reached +1000 mV, the PET channel became less stable and had much larger noise, which made the long-time single channel recording and the followed data analysis more difficult. Therefore, +800 mV instead of +1000 mV was

deemed as the optimum voltage, and utilized for subsequent experiments unless otherwise noted.

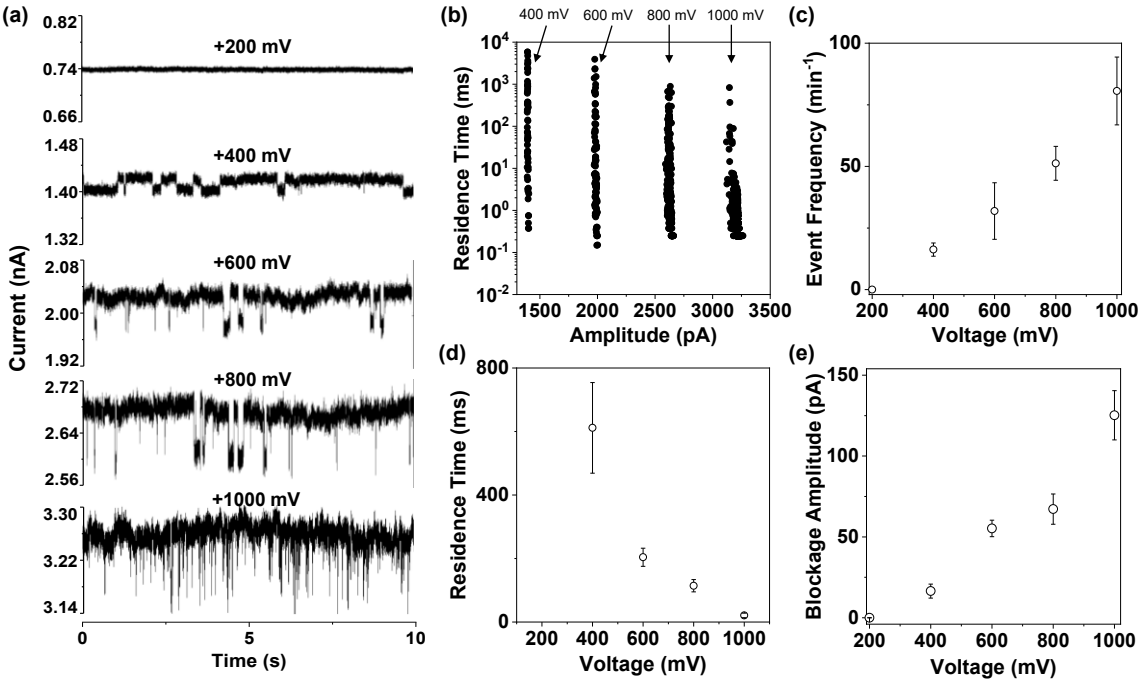

Figure 4. Effect of voltage on detection of HIV-1 protease in the modified PET nanopore. a) Typical 10-s trace segments at various applied voltages; b) the corresponding scatter plots of event residence time vs current blockage amplitude; and plots of c) event frequency, d) residence time and e) blockage amplitude as a function of applied potential. The experiments were performed in a solution comprising 1 M KCl and 10 mM Tris (pH 7.5). The concentration of HIV-1 protease used was 100 ng/mL.

Sensitivity, Selectivity, and Protein Characterization of the PET Nanopore

To determine the sensitivity of our developed PET nanopore sensor for protein detection, the dose response curve for HIV-1 PR was constructed by monitoring the translocation of HIV-1 PR at various concentrations (ranging from 10 ng/mL to 200 ng/mL) in the amine-modified PET nanopore at +800 mV in a 1 M KCl electrolyte buffer solution of pH 7.5. As shown in Figure S5, the frequency of the HIV-1 PR events increased linearly with an increase in the analyte concentration. The limit of detection (LOD) of the nanopore sensor in a 1 min electrical recording was 2.27 ng/mL (equivalent to 210 pM), where LOD was

defined as the concentration of HIV-1 PR corresponding to three times the standard deviation of the blank signal. Such a detection limit, although not as impressive as that of SPR, was comparable with those of other various HIV-1 PR sensors previously reported (Esseghaier et al. 2013; Wang et al. 2014; Zhang et al. 2018), and is good enough for performing HIV-1 PR analysis, where nanomolar concentrations of HIV-1 PR are routinely used (Ingr et al. 2003).

In addition, to examine the selectivity of our modified PET nanopore, three model proteins including trypsin, HSA and BSA, which are frequently used in biomedical research, were selected as potential interfering species. Their interactions with the PET nanopore were investigated under the same experimental condition as that of HIV-1 PR (i.e., at +800 mV, in an electrolyte solution containing 1M KCl and 10 mM Tris (pH 7.5), and in the presence of 100 ng/mL analyte). Our experiments showed that, among the three proteins examined, only trypsin produced ionic current modulations. Since trypsin events had smaller residence time (3.8 ± 1.1 ms versus 114.2 ± 19.4 ms) and blockage amplitude (34.8 ± 5.1 pA versus 67.2 ± 9.3 pA) than those of HIV-1 PR, these two proteins could be well differentiated (Figure S6). Hence, trypsin would not interfere with HIV-1 PR detection. The results are not unreasonable considering that the four proteins (HIV-1 PR, trypsin, HSA, and BSA) have different net charges (Table S1). To be more specifically, at pH 7.5, both HIV-1 PR and trypsin are positively charged (+1.6 and +3.78, respectively), while HSA and BSA are negatively charged (-16.48 and -22.06, respectively). Therefore, under an applied potential bias of +800 mV (note that the nanopore tip side was connected to "ground"), the positively charged protein molecules would be electrophoretically driven through the PET nanopore (from its base to the pore tip), thus causing ionic current modulation events, while negatively charged species would be prevented entering the nanopore. Furthermore, the reason why trypsin had a smaller event residence time than HIV-1 PR was because trypsin had a larger net charge so that it was subjected to a larger electrophoretic force, thus translocating through the nanopore more rapidly. As an important aside, we noticed that, similar to HIV-1 PR, a slight (83 pA) decrease in the open channel current of the PET nanopore would be observed after addition of trypsin to the

electrolyte solution, again indicating that the cationic protein molecules would be absorbed on the interior wall of the nanopore by electrostatic interactions.

Taken together, the above results clearly demonstrated that the net charge of a protein molecule played an important role in its interaction with the amine-modified PET nanopore. One interesting question remaining is whether we can take advantage of proteins' net charges and utilize a combined positively applied potential and negatively applied voltage bias to electrophoretically drive proteins through an amine-modified PET nanopore to differentiate and even characterize protein molecules based on their produced quite different residence time events. For this purpose, the interactions between the PET nanopore and BSA / HSA were investigated at -800 mV (note that no current modulations were observed at +800 mV for these two negatively charged proteins). As we expected, these two proteins indeed produced current blockage events. However, since HSA frequently permanently blocked the PET nanopore so that it was difficult to characterize the signatures of HSA events, translocation of BSA / HSA in the PET nanopore was further carried out at -600 mV. By contrast and in order to obtain the event signatures for all the examined proteins at the same voltage bias, the interaction between the PET nanopore and trypsin was additionally performed at +600 mV. The experimental results were summarized in Figure 5. Clearly, all the proteins (HIV-1 PR, trypsin, BSA, and HSA) produced events with quite different residence time and blockage amplitudes, demonstrating the feasibility of utilizing PET nanopore for rapid differentiation and characterization of proteins.

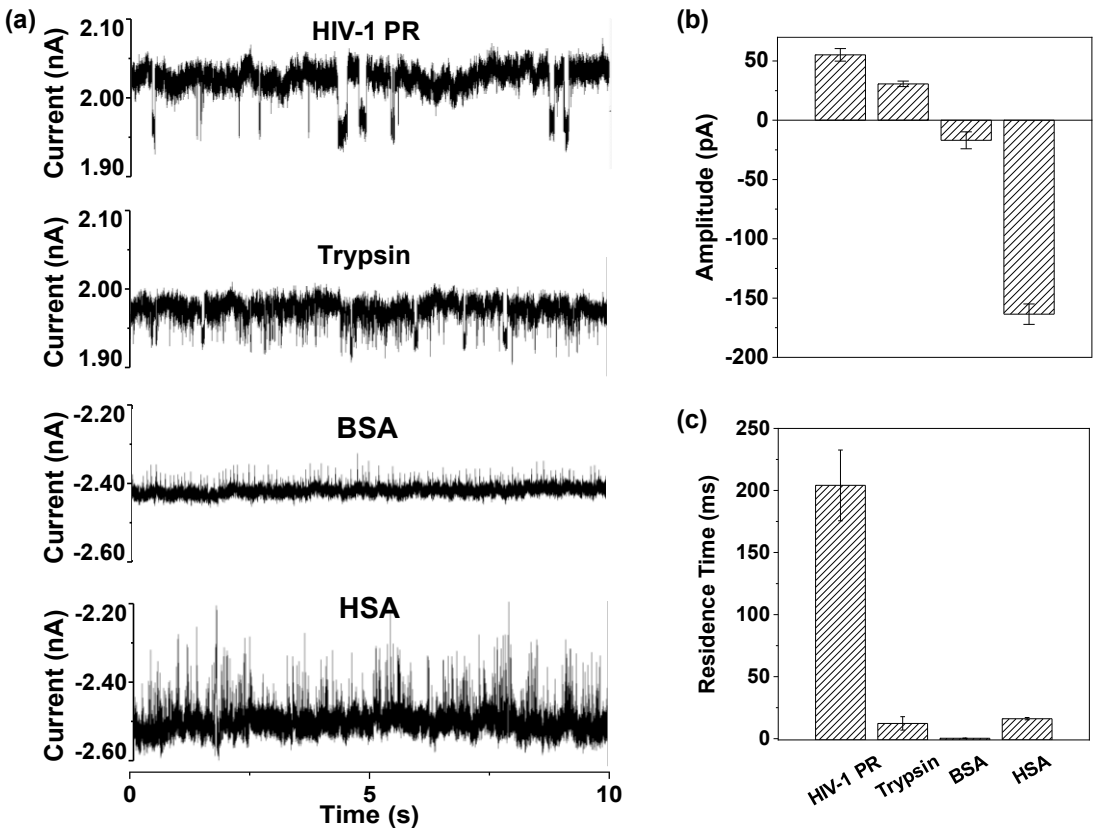

Figure 5. Differentiation and characterization of proteins in the modified PET nanopore. a) Typical trace segments of various proteins in the PET nanopore, and their corresponding event mean (b) blockage amplitude and (c) residence time plots. The experiments were performed at (+)/(-) 600 mV in a solution comprising 1 M KCl and 10 mM Tris (pH 7.5).

Conclusion

In summary, by introducing new functional groups on the inner surface of the *base* side of the PET nanopore, we successfully utilized PET nanopore as a stochastic sensing element for the detection of proteins at the single molecule level. We demonstrate that, by driving the protein molecules into the amine-functionalized PET nanopore base side, we are able to allow for unavoidable molecule adsorption by enhancing desorption of the adsorbed molecules through the creation of a bipolar pore with a higher field, thus achieving both high throughput and long residence time to increase both the resolution and the sensitivity of the nanopore sensor. Our experiments showed that the net charge of a protein played a significant role in the event residence time so that different proteins with different charges could be readily differentiated. Our developed PET nanopore offers the potential for

rapid and label-free protein detection and characterization. In spite of the good limit of detection (2.27 ng/mL), the performance of the PET nanopore protein sensor could be potentially further improved by e.g., employing a salt gradient instead of the symmetrical electrolyte condition used in this work. Our developed PET nanopore sensing strategy not only provides a general platform for exploring fundamental protein dynamics and rapid detection of proteins at the single-molecule level, but also opens new avenues toward advanced deeper understanding of enzymes, development of more efficient biosensing technologies, and constructing novel biomimetic nanopore systems.

ASSOCIATE CONTENT

Supporting Information

Additional table and figures, including properties of proteins, current-voltage (I-V) curves of a single PET conical nanopore between -100 mV and 100 mV, Schematic illustration of the 2-step coupling method for asymmetric modification of the single conical PET nanopore, I-V curves of a single PET conical nanopore at different solution pHs, an uninterrupted 2-min single channel recording trace segment of HIV-1 PR in the amine-modified PET nanopore, and selectivity study of the PET nanopore sensor.

AUTHOR INFORMATION

Corresponding author

*Tel: 312-567-8922. Fax: 312-567-3494. E-mail: xguan5@iit.edu.

Notes

The authors declare no competing financial interests.

Acknowledgments

This work was financially supported by the National Institutes of Health (2R15GM110632-02) and National Science Foundation (1708596).

Reference

Ali, M., Bayer, V., Schiedt, B., Neumann, R., Ensinger, W., 2008. Fabrication and functionalization of single asymmetric nanochannels for electrostatic/hydrophobic association of protein molecules. Nanotechnology 19, 485711.
Ali, M., Nasir, S., Nguyen, Q.H., Sahoo, J.K., Tahir, M.N., Tremel, W., Ensinger, W., 2011a. Metal ion affinity-based biomolecular recognition and conjugation inside synthetic polymer nanopores modified with iron–terpyridine complexes. J. Am. Chem. Soc. 133(43), 17307-17314.
Ali, M., Ramirez, P., Tahir, M.N., Mafe, S., Siwy, Z., Neumann, R., Tremel, W., Ensinger, W., 2011b. Biomolecular conjugation inside synthetic polymer nanopores viaglycoprotein–lectin interactions. Nanoscale 3(4), 1894-1903.
Ali, M., Schiedt, B., Neumann, R., Ensinger, W., 2010. Biosensing with functionalized single asymmetric polymer nanochannels. Macromol. Biosci. 10(1), 28-32.
Bayley, H., 2017. Getting to the bottom of the well. Nat. Nanotechnol. 12(12), 1116-1117.
Bovey, F.A., 1961. Nuclear magnetic resonance spectroscopy of proteins: the hydrogen bonding of water in bovine serum albumin solutions. Nature 192(4800), 324-326.
Branton, D., Deamer, D.W., Marziali, A., Bayley, H., Benner, S.A., Butler, T., Di Ventra, M., Garaj, S., Hibbs, A., Huang, X., Jovanovich, S.B., Krstic, P.S., Lindsay, S., Ling, X.S., Mastrangelo, C.H., Meller, A., Oliver, J.S., Pershin, Y.V., Ramsey, J.M., Riehn, R., Soni, G.V., Tabard-Cossa, V., Wanunu, M., Wiggin, M., Schloss, J.A., 2008. The potential and challenges of nanopore sequencing. Nat. Biotechnol. 26(10), 1146-1153.
Cervera, J., Schiedt, B., Neumann, R., Mafé, S., Ramírez, P., 2006. Ionic conduction, rectification, and selectivity in single conical nanopores. The Journal of Chemical Physics 124(10), 104706.
Chen, X., M. Roozbahani, G., Ye, Z., Zhang, Y., Ma, R., Xiang, J., Guan, X., 2018. Label-free detection of dna mutations by nanopore analysis. ACS Appl. Mater. Interfaces 10(14), 11519-11528.
Chen, X., Zhang, Y., Mohammadi Roozbahani, G., Guan, X., 2019. Salt-mediated nanopore detection of ADAM-17. ACS Applied Bio Materials 2(1), 504-509.
Choi, Y., Baker, L.A., Hillebrenner, H., Martin, C.R., 2006. Biosensing with conically shaped nanopores and nanotubes. Phys. Chem. Chem. Phys. 8(43), 4976-4988.
Chuah, K., Wu, Y., Vivekchand, S.R.C., Gaus, K., Reece, P.J., Micolich, A.P., Gooding, J.J., 2019. Nanopore blockade sensors for ultrasensitive detection of proteins in complex biological samples. Nature Communications 10(1), 2109.
Deamer, D., Akeson, M., Branton, D., 2016. Three decades of nanopore sequencing. Nat. Biotechnol. 34(5), 518-524.
Esseghaier, C., Ng, A., Zourob, M., 2013. A novel and rapid assay for HIV-1 protease detection using magnetic bead mediation. Biosensors and Bioelectronics 41(Supplement C), 335-341.
García-Chamé, M.-Á., Gutiérrez-Sanz, Ó., Ercan-Herbst, E., Haustein, N., Filipiak, M.S., Ehrnhöfer, D.E., Tarasov, A., 2020. A transistor-based label-free immunosensor for rapid detection of tau protein. Biosensors and Bioelectronics 159, 112129.
Greenfield, N.J., 2006. Using circular dichroism spectra to estimate protein secondary structure. Nat. Protoc. 1(6), 2876-2890.
Heerema, S.J., Dekker, C., 2016. Graphene nanodevices for DNA sequencing. Nat. Nanotechnol. 11(2), 127-136.
Henrickson, S.E., Misakian, M., Robertson, B., Kasianowicz, J.J., 2000. Driven DNA transport into an asymmetric nanometer-scale pore. Phys. Rev. Lett. 85(14), 3057-3060.
Hou, X., Guo, W., Xia, F., Nie, F.-Q., Dong, H., Tian, Y., Wen, L., Wang, L., Cao, L., Yang, Y., Xue, J., Song, Y., Wang, Y., Liu, D., Jiang, L., 2009. A biomimetic potassium responsive nanochannel: G-quadruplex DNA conformational switching in a synthetic nanopore. J. Am. Chem. Soc. 131(22), 7800-7805.
Ilkhani, H., Sarparast, M., Noori, A., Zahra Bathaie, S., Mousavi, M.F., 2015. Electrochemical aptamer/antibody based sandwich immunosensor for the detection of EGFR, a cancer biomarker, using gold nanoparticles as a signaling probe. Biosensors and Bioelectronics 74, 491-497.
Ingr, M., Uhlíková, T.á., Střížovský, K., Majerová, E., Konvalinka, J., 2003. Kinetics of the dimerization of retroviral proteases: The “fireman’s grip” and dimerization. Protein Science : A Publication of the Protein Society 12(10), 2173-2182.
Karawdeniya, B.I., Bandara, Y.M.N.D.Y., Nichols, J.W., Chevalier, R.B., Dwyer, J.R., 2018. Surveying silicon nitride nanopores for glycomics and heparin quality assurance. Nature Communications 9(1), 3278.

Keskin, O., Tuncbag, N., Gursoy, A., 2016. Predicting Protein–protein interactions from the molecular to the proteome level. Chem. Rev. (Washington, DC, U. S.) 116(8), 4884-4909.
Plesa, C., Kowalczyk, S.W., Zinsmeester, R., Grosberg, A.Y., Rabin, Y., Dekker, C., 2013. Fast translocation of proteins through solid state nanopores. Nano Lett. 13(2), 658-663.
Roman, J., Jarroux, N., Patriarche, G., Français, O., Pelta, J., Le Pioufle, B., Bacri, L., 2017. Functionalized solid-state nanopore integrated in a reusable microfluidic device for a better stability and nanoparticle detection. ACS Appl. Mater. Interfaces 9(48), 41634-41640.
Roozbahani, G.M., Zhang, Y., Chen, X., Soflaee, M.H., Guan, X., 2019. Enzymatic reaction-based nanopore detection of zinc ions. Analyst 144(24), 7432-7436.
Sexton, L.T., Horne, L.P., Sherrill, S.A., Bishop, G.W., Baker, L.A., Martin, C.R., 2007. Resistive-pulse studies of proteins and protein/antibody complexes using a conical nanotube sensor. J. Am. Chem. Soc. 129(43), 13144-13152.
Shim, J., Rivera, J.A., Bashir, R., 2013. Electron beam induced local crystallization of HfO_2 nanopores for biosensing applications. Nanoscale 5(22), 10887-10893.
Siwy, Z.S., Davenport, M., 2010. Graphene opens up to DNA. Nat. Nanotechnol. 5(10), 697-698.
Slonkina, E., Kolomeisky, A.B., 2003. Polymer translocation through a long nanopore. The Journal of Chemical Physics 118(15), 7112-7118.
Smyth, M.S., Martin, J.H., 2000. x ray crystallography. Mol Pathol 53(1), 8-14.
Storm, A.J., Chen, J.H., Zandbergen, H.W., Dekker, C., 2005. Translocation of double-strand DNA through a silicon oxide nanopore. Physical Review E 71(5), 051903.
Talaga, D.S., Li, J., 2009. Single-molecule protein unfolding in solid state nanopores. J. Am. Chem. Soc. 131(26), 9287-9297.
Vlassiouk, I., Kozel, T.R., Siwy, Z.S., 2009. Biosensing with nanofluidic diodes. J. Am. Chem. Soc. 131(23), 8211-8220.
Vlassiouk, I., Siwy, Z.S., 2007. Nanofluidic diode. Nano Lett. 7(3), 552-556.
Wang, C., Fu, Q., Wang, X., Kong, D., Sheng, Q., Wang, Y., Chen, Q., Xue, J., 2015. Atomic layer deposition modified track-etched conical nanochannels for protein sensing. Anal. Chem. 87(16), 8227-8233.
Wang, G., Zhao, Q., Kang, X., Guan, X., 2013. Probing mercury(II)–DNA interactions by nanopore stochastic sensing. The Journal of Physical Chemistry B 117(17), 4763-4769.
Wang, L., Chen, X., Zhou, S., Roozbahani, G.M., Zhang, Y., Wang, D., Guan, X., 2018. Displacement chemistry-based nanopore analysis of nucleic acids in complicated matrices. Chem. Commun. (Cambridge, U. K.) 54(99), 13977-13980.
Wang, L., Han, Y., Zhou, S., Guan, X., 2014. Real-time label-free measurement of HIV-1 protease activity by nanopore analysis. Biosensors and Bioelectronics 62, 158-162.
White, H.S., Bund, A., 2008. Ion current rectification at nanopores in glass membranes. Langmuir 24(5), 2212-2218.
Xie, S., Moya, C., Bilgin, B., Jayaraman, A., Walton, S.P., 2009. Emerging affinity-based techniques in proteomics. Expert Review of Proteomics 6(5), 573-583.
Yan, Y., Wang, L., Xue, J., Chang, H.-C., 2013. Ion current rectification inversion in conic nanopores: Nonequilibrium ion transport biased by ion selectivity and spatial asymmetry. The Journal of Chemical Physics 138(4), 044706.
Zhang, W., Tang, S., Jin, Y., Yang, C., He, L., Wang, J., Chen, Y., 2020. Multiplex SERS-based lateral flow immunosensor for the detection of major mycotoxins in maize utilizing dual Raman labels and triple test lines. J. Hazard. Mater. 393, 122348.
Zhang, Y., Chen, X., Roozbahani, G.M., Guan, X., 2018. Graphene oxide-based biosensing platform for rapid and sensitive detection of HIV-1 protease. Anal. Bioanal. Chem. 410(24), 6177-6185.
Zhang, Y., Chen, X., Roozbahani, G.M., Guan, X., 2019. Rapid and sensitive detection of the activity of ADAM17 using a graphene oxide-based fluorescence sensor. Analyst 144(5), 1825-1830.

Scheme 1

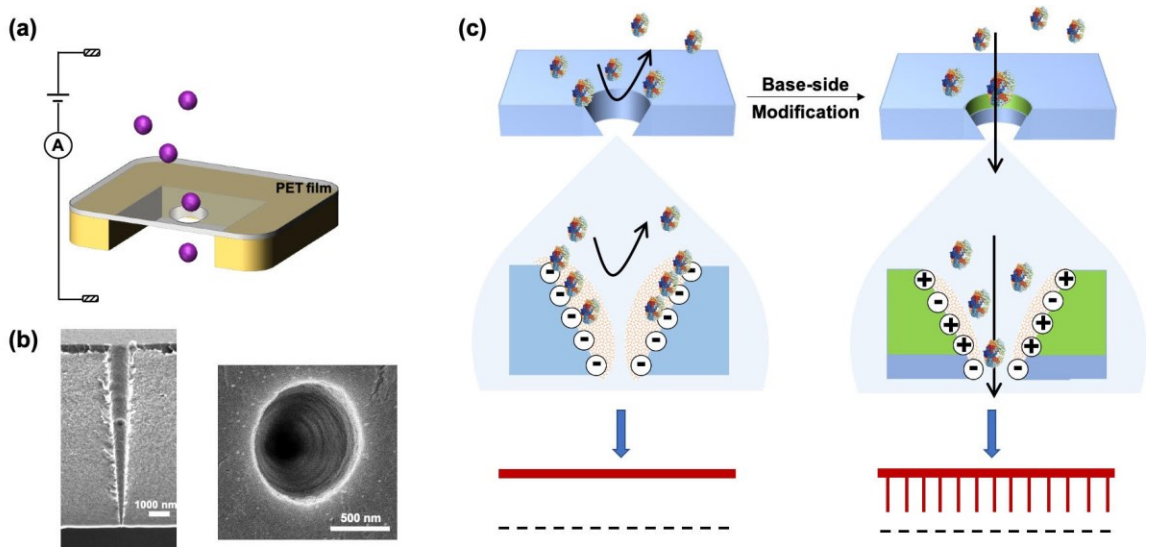

Scheme 1. The principle of a modified single conical PET nanopore for detection of proteins. (a) Schematic representation of the PET nanopore sensing system; (b) Representative cross-sectional SEM image and top view of a conical nanopore; (c) Before modification of the PET nanopore, protein molecules could not pass through the nanopore due to the large energy barrier, and some protein molecules might be absorbed on the interior wall of the nanopore by electrostatic and hydrophobic interactions. In contrast, asymmetric modification of the nanopore *base* produces a new type of surface and property in the interior wall of the nanopore, which reduces the energetic barrier for proteins' entrance into the pore and slows down the velocity of ion flux, resulting in ionic current blockage events.

Figure 1

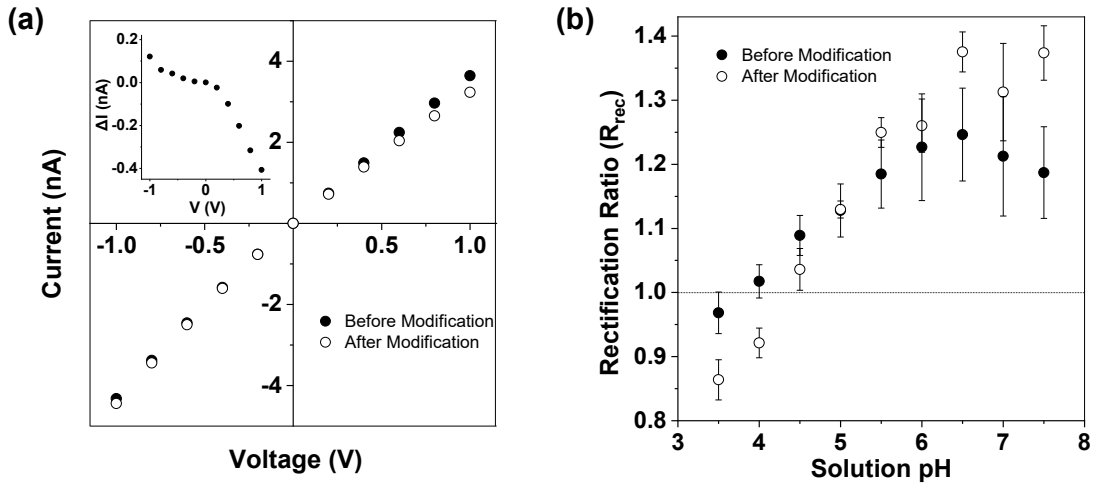

Figure 1. Modification of a single conical PET nanopore. (a) Current-voltage (I-V) curves before and after chemical modification. The inset in Fig. 1a displayed the change in the ionic current before and after nanopore modification. Experiments were performed in a solution containing 1 M KCl and 1 mM EDTA (pH 7.5). The base side of the PET nanopore was modified in 0.1 M MES (pH 6.0), 0.05 M EDC/0.2 M Sulfo-NHS, and 0.05 M ethylenediamine. The diameters of the nanopore tip and base are ~ 5.6 nm and 1000 nm, respectively. (b) Plot of rectification ratio (R_{rec}) as a function of solution pH. The values of R_{rec} were measured at 1 V. The current-voltage curve flipped at the value of pH that corresponds to the film isoelectric point (pI). The value of pI was ~4.3 for the amine-modified PET pore and ~3.8 for the unmodified one, with no rectification at this point.

Figure 2

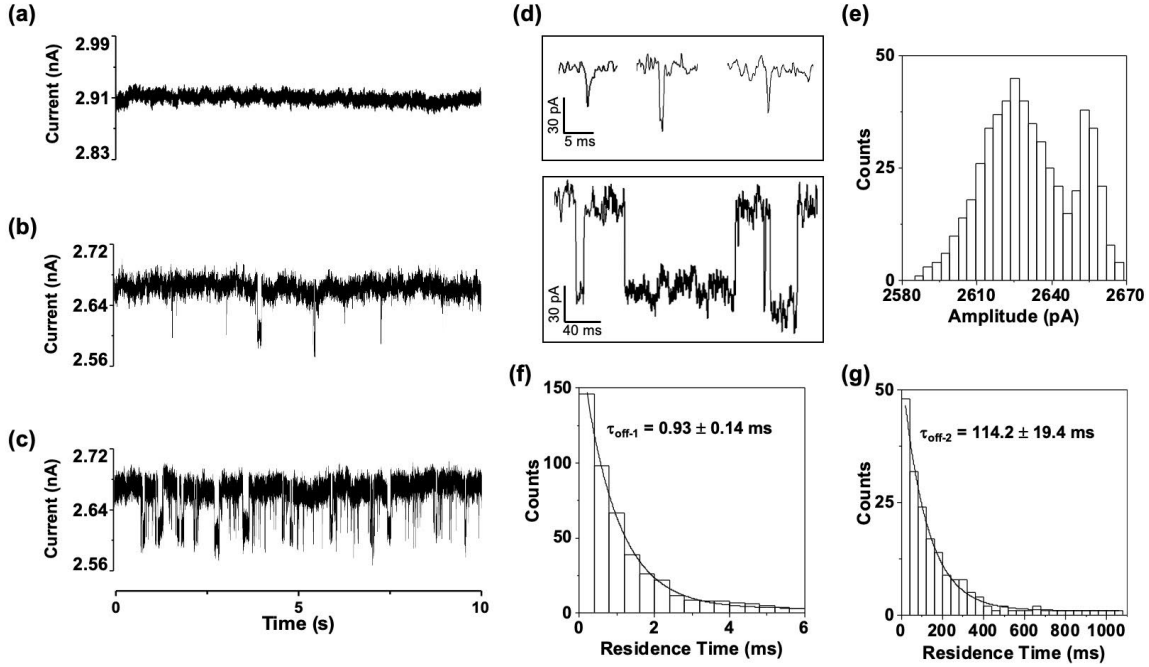

Figure 2. Detection of HIV-1 protease in a PET nanopore. Typical 10-s single channel recording trace segments of a) 100 ng/mL HIV-1 protease in the unmodified PET nanopore, b) 10 ng/mL and c) 100 ng/mL HIV-1 protease in the amine-modified PET nanopore; d) selective individual short-lived and long-lived events; and the corresponding event (e) amplitude histogram and residence time histograms of (f) short-lived and (g) long-lived events of Figure 2c. The experiments were performed at +800 mV in a solution comprising 1 M KCl and 10 mM Tris (pH 7.5). An uninterrupted 2-min single-channel recording trace of 100 ng/mL HIV-1 PR in the modified PET nanopore was displayed in Figure S4.

Figure 3

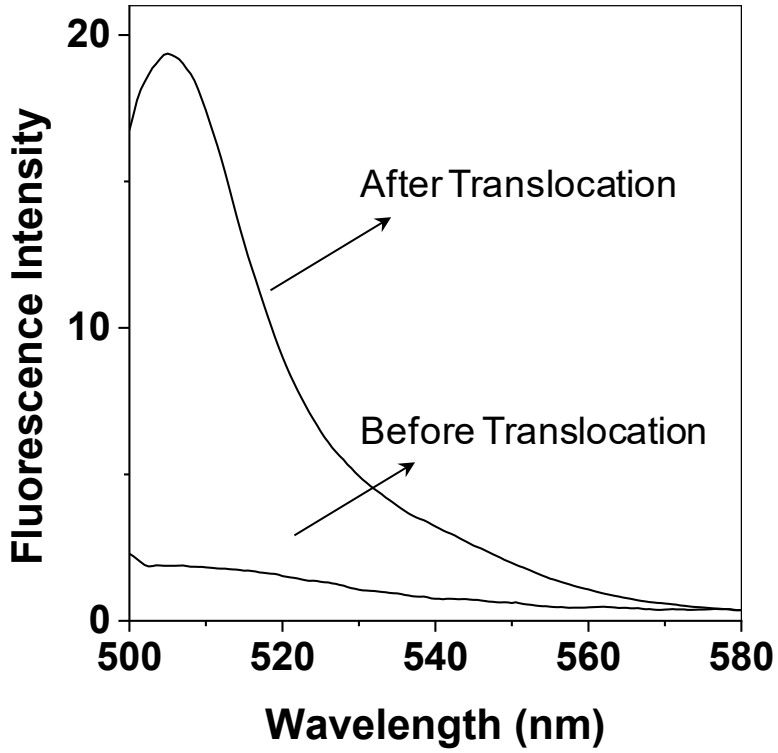

Figure 3. Fluorescence intensity of the nanopore *tip*-side compartment solution before and after 3-h eGFP translocation in the modified PET nanopore. The experiment was performed at +800 mV with 100 ng/mL of eGFP added to the *base* side of the modified nanopore bathed in a pH 5.0 electrolyte solution comprising 1 M KCl and 10 mM Tris. The fluorescence spectrum was obtained with $\lambda_{ex/em}$ = 488/507 nm at room temperature.

Figure 4

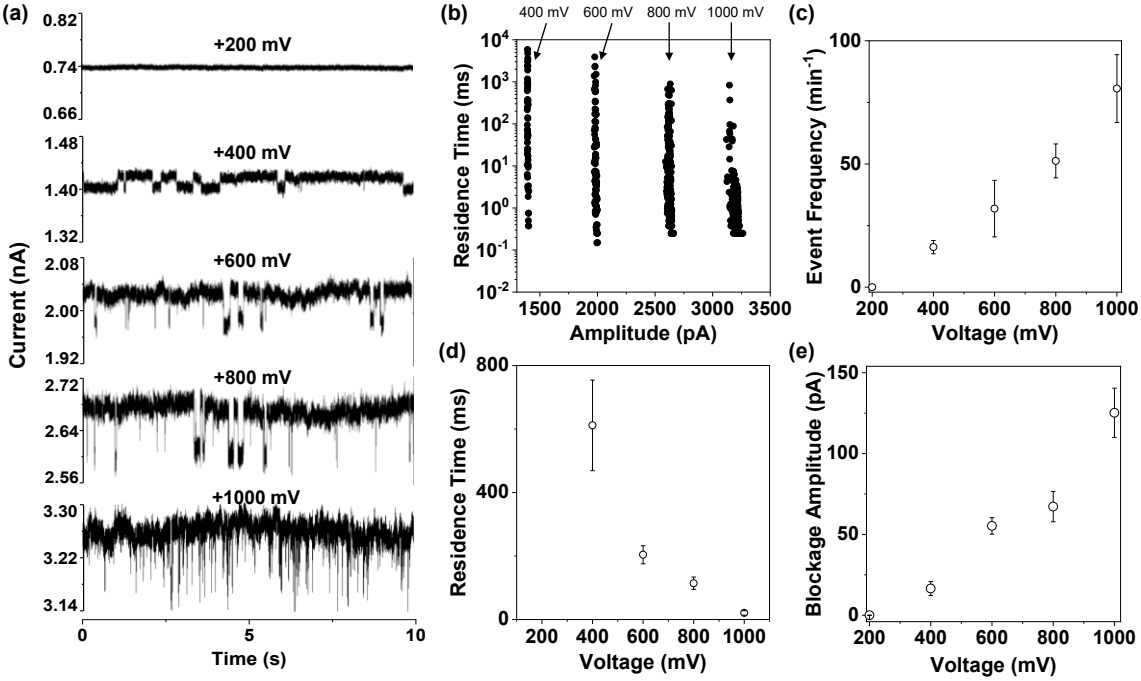

Figure 4. Effect of voltage on detection of HIV-1 protease in the modified PET nanopore. a) Typical 10-s trace segments at various applied voltages; b) the corresponding scatter plots of event residence time vs current blockage amplitude; and plots of c) event frequency, d) residence time and e) blockage amplitude as a function of applied potential. The experiments were performed in a solution comprising 1 M KCl and 10 mM Tris (pH 7.5). The concentration of HIV-1 protease used was 100 ng/mL.

Figure 5

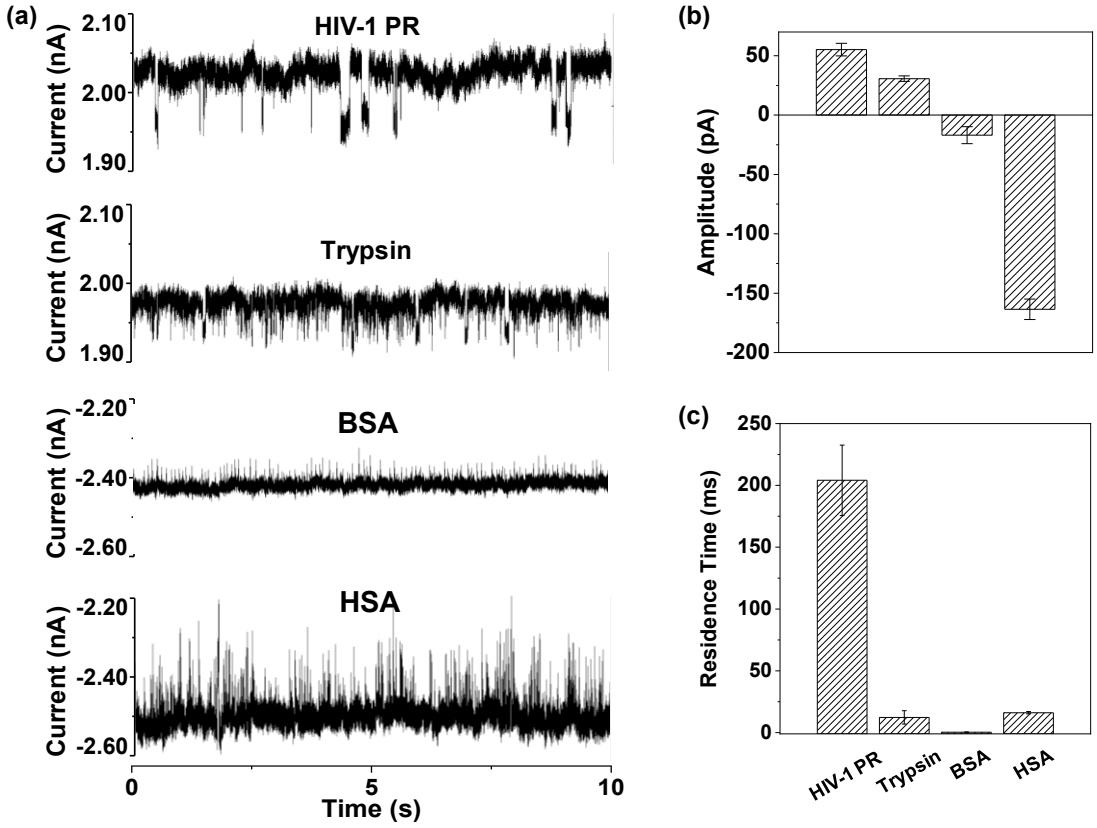

Figure 5. Differentiation and characterization of proteins in the modified PET nanopore. a) Typical trace segments of various proteins in the PET nanopore, and their corresponding event mean (b) blockage amplitude and (c) residence time plots. The experiments were performed at (+)/(-) 600 mV in a solution comprising 1 M KCl and 10 mM Tris (pH 7.5).